

# Development of drug loaded silver nanoparticle composite chitosan film for burn wound healing

Kishorkumar SORATHIA<sup>1\*</sup>, Margi BHUT<sup>1</sup>, Vanshika PATEL<sup>1</sup>, Gautami UBHARANI<sup>1</sup>,  
Krutagn PATEL<sup>1</sup>, Tejal SONI<sup>1</sup>, Mehul PATEL<sup>1</sup>

<sup>1</sup> Department of Pharmaceutics, Faculty of Pharmacy, Dharmsinh Desai University, Nadiad, India.

\* Corresponding Author. E-mail: [krsorathia@yahoo.com](mailto:krsorathia@yahoo.com) (K.S.); Tel. +91-942-637 60 56.

Received: 9 April 2024 / Revised: 5 August 2024 / Accepted: 8 August 2024

**ABSTRACT:** In this study, a novel topical film for burn wound infections was developed by combining chitosan, silver nanoparticles, and the antimicrobial drug neomycin sulfate. Chitosan, a natural polymer, was chosen for its biodegradability, biocompatibility, and antibacterial properties. Silver nanoparticles exhibited bactericidal effects against various Gram-negative and Gram-positive bacteria, while neomycin sulfate is an antimicrobial drug. The silver nanoparticles were synthesized and characterized using UV spectroscopy, dynamic light scattering, and zeta potential. A film was formed on surgical dressing material containing chitosan, silver nanoparticles, and neomycin sulfate and evaluated for *in-vitro* anti-microbial activity and *in-vivo* wound healing activity on rat model. Antimicrobial activity of film showed significant differences compared to chitosan solution, silver nanoparticles, and neomycin sulfate. X-ray diffraction and FT-IR data suggested that the drug and formulation were in an amorphous form, with no interactions between the drug and excipient. The wound healing properties of neomycin sulfate-loaded silver nanoparticle-chitosan film were significantly higher than chitosan film, silver nanoparticle-containing chitosan film, and silver sulfadiazine ointment (Burn cool). Notably, the neomycin sulfate-loaded silver nanoparticle-chitosan film have significantly enhanced wound healing and can be a potential alternative in treatment of burn wound.

**KEYWORDS:** Antimicrobial activity; chitosan; neomycin sulphate; silver nanoparticle; wound healing.

## 1. INTRODUCTION

Burns are tissue injury that can be brought on by a variety of factors, including heat, chemicals, sunlight, and nuclear radiation. Because the skin has an abundance of sensory nerve endings that can detect a wide range of external physical and chemical stimuli, it serves as the body's exterior barrier. The epidermis and dermis are the two distinct layers that make up the skin. Most layers are destroyed in severe burn wounds, which might affect skin functions. The most prevalent type of burn injuries are thermal burns, which account for around 86% of injured patients requiring admission to a burn center. These burns can arise from steam, hot fluids, electrical injury, fire or sparkle, etc. Burns due to scalds are the next most common. The treatment for burn wounds depends on the depth of injury. Wound healing is a process of repairing the injury caused. It is a complex series of interactions that occur in the different cells, cytokine mediators, and the extracellular matrix. In most cases of burn, only the skin is affected and the treatments includes povidone-iodine, silver sulfadiazine, etc [1,2].

Neomycin sulphate, widely applied topically, is an aminoglycoside antibiotic that is antimicrobial and inhibits bacterial growth by attaching to the 30S ribosomal subunit and causing t-RNA to be misread. It is widely used as topical preparations for wound and other dermal infections [3,4]. Silver holds an ancient record of use in medicine and hygiene because of its broad-spectrum antimicrobial activity against bacteria, fungi and algae. Silver has been used in its nanoparticulate form since a number of years. Products consisting nanosilvers are the most important class of nanoproducts. The increasing and widespread use of nanosilver in inhibiting the bacterial growth has gained the attraction of researchers as, the growth of silver-resistant bacteria is pushed by low levels of silver ions. Silver nitrate and silver sulfadiazine were frequently used for the treatment of superficial and deep cutaneous burns or wounds, as well as the eradication of warts [5]. A little dose (in ppm) of silver nanoparticles (AgNPs) is sufficient for the activity, and it takes more time for microorganisms to develop a resistance to them [6]. The mechanism of action of silver was thought

**How to cite this article:** Sorathia K, Bhut M, Patel V, Ubharani G, Patel K, Soni T, Patel M. Development of drug loaded silver nanoparticle composite chitosan film for burn wound healing. J Res Pharm. 2025; 29(3): 1154-1167.

to be dependent on Ag<sup>+</sup> ions, which impede bacterial growth by splashing respiratory enzymes and electron transport system components through interference with DNA activity [7,8]. Silver nanoparticles work in combination with antibiotics to enhance their effects [9]. Numerous research have demonstrated that nanosilver has bactericidal effects on both Gram-negative and Gram-positive bacteria, although the exact mechanism of action is still unclear. The antibacterial activity of AgNPs against Gram-negative bacteria like *E. coli*, *V. cholera*, *P. aeruginosa*, and *S. typhi*, has suggested that the surface of the cell membrane receives the attachment of the AgNPs, which penetrate the bacteria, affect its functions, and release the silver ions. The similar activity was also witnessed in some gram positive bacteria like *B. subtilis*, *S. aureus*, and *E. Faecalis* [7, 10,11]. It was also found that some drug resistant bacteria also receives antibacterial action through silver nanoparticles [12]. A number of methods are utilised for preparing the AgNPs from solution of silver nitrate (AgNO<sub>3</sub>) such as chemical reduction method and ultraviolet method [13].

Chitosan is a glucosamine (2-amino-2-deoxy-D-glucose) and N-acetyl glucosamine polymer that is β-1,4-linked. It is a polymer of poly N acetyl glucosamine, a chitin derivative that ranks second in biopolymer abundance to cellulose [14]. Chitosan has been approved recently in the USA for use in bandages and other hemostatic treatments due to its ability to bond with red blood cells and has the ability to quickly coagulate blood [15]. As a semipermeable biological dressing, it preserves sterile wound exudate beneath a dry scab, limiting dehydration and contamination of the wound, and promoting the best possible healing conditions [16,17]. Chitosan is a biodegradable, biocompatible, and non-toxic polymer [18-22]. It is utilised in orthopaedics, wound healing, ophthalmology, bone healing, cell delivery systems, and drug delivery [23]. It has antibacterial effects on yeast, fungus, and bacteria. It exhibits hypoallergenic, hemostatic, quick blood clotting, and fat-attractive properties through attaching to dietary lipids [24]. In spite of lots of research and developments in this topic, the precise processes underlying chitosan's antibacterial effects remain unknown [16, 17, 25-27].

Depending on the type of wound, a different dressing material is needed, one with the right fluid absorption, healing period, and mechanical strength. Polymeric wound dressings are used in a relatively novel method of wound healing to deliver different medicinal agents that can actively participate in one or more phases of the wound healing process. When these compounds' actions are combined with the dressing's physical qualities, the rate of wound healing can be improved [28]. The present work was aimed to develop neomycin sulphate loaded silver nanoparticle composite chitosan film for better wound healing. The combination of antimicrobial agents along with silver nanoparticles and chitosan may improve wound healing.

## 2. RESULTS AND DISCUSSION

### 2.1. Synthesis of silver nanoparticle using UV method

In this technique, the UV light was used as a reducing agent. The UV process takes a lot longer than the chemical method to complete. Particle size, zeta potential, and UV measurements are represented in Table 1. The results indicated stable and uniform formation of AgNPs. The produced silver nanoparticles have a very low zeta potential and a small particle size, and they can only be obtained for up to 48 hours before they begin to aggregate. Silver nanoparticles shown a distinctive peak at about 420 nm while analysed through UV-visible spectrophotometer.

**Table 1.** Characteristics of silver nanoparticle synthesized by UV method

Time (Hr)	Particle size (nm)	Absorbance	Zeta potential (mV)
1	102.9±0.321	0.371±0.002	-4.06±0.030
4	112.8±0.916	1.139±0.002	-4.36±0.077
6	106.9±0.416	1.214±0.007	-3.14±0.068
20	76.28±0.914	2.316±0.005	-3.12±0.020
24	71.17±0.775	2.710±0.012	-3.05±0.066
30	71.10±0.960	2.838±0.005	-2.45±0.041
48	70.51±0.745	3.147±0.008	-1.63±0.080

### 2.2. Synthesis of silver nanoparticle using chemical method

Chemical approach is significantly superior to UV method of synthesis due to its advantages including less time-consuming (1 hour) and without the need of a sterile environment and produce smaller

particle size as compared to UV technique. Different surfactants were used to obtain silver nanoparticles and results are depicted in Table 2.

**Table 2.** Characteristics of synthesized silver nanoparticle by chemical method using different surfactant

Surfactant (1% w/v)	Particle size (nm)	Zeta potential (mV)	Absorbance
Dodecyl trimethyl ammonium bromide (D-TAB)	572.1±4.275	-32.8±1.479	-
Cetyl trimethyl ammonium bromide (C-TAB)	399.3±6.300	21.8±1.123	-
Sodium dodecyl sulphate (SDS)	76.43±2.543	-55.9±1.457	0.349±0.005
Span 20	342.7±8.212	-12.1±0.529	-
Tween 80	226.9±5.020	-34.2±5.288	0.215±0.006
Brij 35	118.8±5.056	-17.3±2.351	0.194±0.005

When compared to other surfactants such as dodecyl trimethyl ammonium bromide, cetyl trimethyl ammonium bromide, span 20, tween 80, and brij 35, the sodium dodecyl sulphate (SDS) produced silver nanoparticles with smaller particle size, more stable particles, and more yield. Among several surfactants, SDS produces good results, hence it was selected for the further development of AgNPs and its concentration was optimized. For the optimization different concentration of SDS like 5, 25, 35, 50, 100, 200 mM were used for synthesis. The characteristics of synthesized silver nanoparticles like particle size, UV, and zeta potential are detailed in Table 3. As per results, the concentration of SDS has greater effect on characteristics of silver nanoparticles. From the results, it is clear that a concentration of 50mM produces the best results, which include smaller particle sizes, higher amounts of particles and high zeta potential.

**Table 3.** Characteristics of synthesised silver nanoparticles using different concentrations of sodium dodecyl sulphate.

Concentration used (mM)	Particle size (nm)	Zeta potential (Mv)	Absorbance
5	100.4±4.085	-91.9±7.054	0.081±0.009
25	79.47±1.679	-60±5.052	0.263±0.011
35	76.43±3.309	-55.9±9.600	0.349±0.009
50	49.07±2.170	-73.6±8.271	0.499±0.017
100	40.79±2.468	-75.6±5.944	0.138±0.013
200	295.6±2.302	-55.7±4.728	0.104±0.015

Further, effect of different polymers on synthesis of silver nanoparticles was determined using HPMC K4M, PVP K30, and  $\beta$ -cyclodextrin. The results of parameters like particle size, UV absorbance and zeta potential are shown in Table 4. In comparison to HPMC K4M and  $\beta$ -CD, PVP K30 produced nanoparticles with smaller particle sizes (60.78  $\pm$ 3.870), higher yield of particles, and extremely stable (higher zeta potential) -56.4  $\pm$ 2.870 mV particles. So, PVP K30 was selected for the preparation of silver nanoparticles. The optimized silver nanoparticles were prepared utilizing SDS at concentration of 50 mM as surfactant and PVP K30 0.1 % w/v as polymer.

**Table 4.** Characteristics of silver nanoparticles prepared using different polymers

Polymer (0.1% w/v)	Particle size	Zeta potential(mV)	Absorbance
Polyvinyl Pyrrolidone K30	60.78±3.870	-56.4±2.563	0.442±0.013
Hydroxyl propyl methyl cellulose K4M	110.6±5.105	-8.28±1.644	0.199±0.010
$\beta$ -cyclodextrin	101.7±8.730	-15.4±1.401	0.937±0.012

Thus, AgNPs prepared with SDS (50 mM) and PVP K30 (0.1%) has smaller particle size and higher stability as indicated by zeta potential. This can be attributed to the transportation of electrostatically bonded Ag<sup>+</sup> ions to the growing surface by SDS monomers and submicellar aggregates, resulting in stable AgNPs.(29) Presence of the micelles around the AgNPs inhibits the approach of Ag<sup>+</sup> ions to the AgNPs and their coalescence. Consequently of the capping of micelles/monomers around the nucleus of AgNPs in the presence of SDS and the limited number of monomer aggregates, may results into smaller size distribution and greater stability of AgNPs [29,30]. Role of PVP K30 in nanoparticles is a surface stabilizer, growth

modulator, nanoparticle dispersant, and reducing agent. This might be result of PVP K-30's stronger interactions with positively charged silver ions during the reduction process due to its increased tendency to give electrons. Consequently, it is expected that the surfaces of the capping molecules and nanoparticles will stabilize more efficiently [31].

### 2.3. Preparation of Chitosan Film on Surgical dressing material

Films were formed using different chitosan concentrations varying from 1% to 2% as shown in Table 5. Different concentration of chitosan was present in the drug loaded silver nanoparticle film prepared on surgical dressing material. The film surface parameters like film forming capacity, surface smoothness, etc. were evaluated after drying the film in the oven for 3-4 hours at 60°C for determining the optimum chitosan concentration for the film formation. As per the results depicted in Table 5, the Film formed at 1.4% chitosan concentration showed the best results. The film formed has the best film forming capacity along with the smooth surface. Thus, 1.4 % of chitosan concentration was selected for the final formulation.

**Table 5.** Surface properties of chitosan films

Batch	Chitosan concentration	Film surface properties*
C1	1.0%	-
C2	1.2%	++
C3	1.4%	+++
C4	1.6%	++
C5	1.8%	-
C6	2.0%	-

\*- Indicates no film formation; ++ indicates film form but not smooth; +++ indicates smooth film formation

### 2.4. Evaluation of drug loaded silver nanoparticle-chitosan film

The films were further evaluated for drug content, thickness and water absorption capacity. The thickness of the film was found to be 1.114±0.012 mm while drug content was 97.599±1.151 % which indicates sufficient drug loading ability of the film. Water absorption capacity of the film is shown in Table 6. The results are indication of great ability of the film for absorption of the serous drainage from the wound as a normal part of wound healing process and which otherwise may hinder the wound healing.

**Table 6.** Water absorption capacity of various chitosan films

Sr. No	Time (Hour)	Blank chitosan film	Silver nanoparticle-Chitosan film	Drug loaded Silver nanoparticle-Chitosan film
1	0.5	1000.52± 0.307	997.79± 0.324	548.68±0.321
2	1	1117.99± 0.265	1060.69± 0.287	987.26±0.407
3	1.5	1176.45± 0.289	1146.85± 0.211	1005.88±0.89
4	2	1254.23± 0.213	1211.67±0.197	1109.67±0.654
5	3	1375.13± 0.167	1320.44±0.243	1234.32±0.921
6	24	1579.10± 0.215	1505.97±0.178	1398.11±0.786

### 2.5. Antimicrobial activity

Results of the antimicrobial activity are shown in Table 7 indicating zone of inhibition of different formulation for Gram-positive bacteria *S. aureus* and Gram-negative bacteria *E. coli*. Results are clear indication of enhancement of antimicrobial activity of the drug loaded silver nanoparticle-chitosan film compared to drug, silver nanoparticles and chitosan alone as well as combinations of them. This could be attributed to synergistic activity of drug-silver nanoparticle-chitosan combination. This enhanced antimicrobial activity would also be responsible for enhancement of the wound healing activity.

**Table 7.** Antimicrobial study of different formulations

Microorganism	Zone of Inhibition (mm)						
	Control (Distilled water)	Silver-nanoparticle	Chitosan	Neomycin Sulphate	Neomycin + Silver nanoparticle	Chitosan+ Silver nanoparticle	Neomycin loaded Chitosan- Silver nanoparticle film
Staphylococcus aureus	-	14.0±0.09	9.0±0.034	11±0.038	21±0.047	13±0.052	35±0.041
Escherichia coli	-	14.0±0.05	7.0±0.031	5±0.02	21±0.043	15±0.056	29±0.04

## 2.6. *In vitro* drug release Profile

Figure 1 depicts the percentage cumulative drug release from an *in vitro* drug release study performed on drug loaded silver nanoparticle-chitosan film on dressing. The plot shows that it takes more than 7 h to release 80 % of drug from the dressing indicating sustained release of drug for sufficient period of time exerting prolonged duration of action.

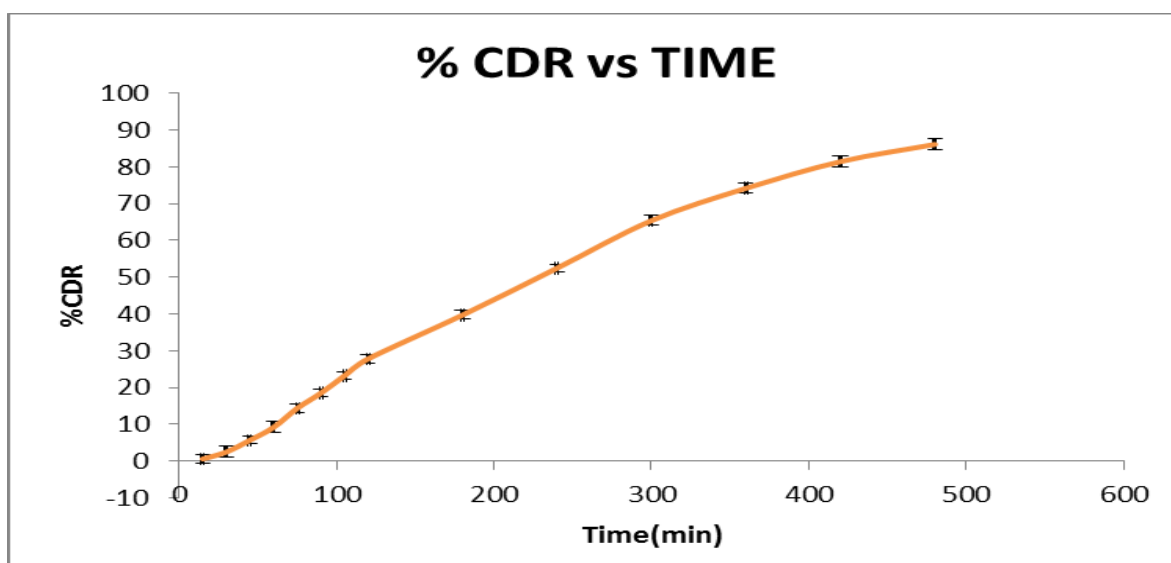


**Figure 1.** *In vitro* drug release profile from drug loaded silver nanoparticle-chitosan film dressing.

## 2.7. X-Ray Diffraction (XRD)

XRD spectra of neomycin sulphate and film dressing formulation were represented in Figure 2. It indicates that the drug as well as neomycin sulphate loaded silver nanoparticle composite chitosan film both are in amorphous form. XRD spectra of formulation shows the change in the intensity of peak which may be attributed to the amorphization of drug due to complex formation between neomycin sulphate, silver nanoparticle and chitosan.

## 2.8. Fourier Transport Infrared Spectroscopy (FT-IR)

FT-IR spectra of neomycin and optimized formulation are represented in figure 3. In FT-IR spectra of both neomycin and drug loaded silver nanoparticle composite chitosan film optimized formulation, absorption bands were observed at 2962 cm<sup>-1</sup>, 2854 cm<sup>-1</sup> (C-H stretching), 1770 cm<sup>-1</sup> (C=O stretching), 1480 cm<sup>-1</sup> (C-H bending) and 1259 cm<sup>-1</sup>, 1091 cm<sup>-1</sup>, 1022 cm<sup>-1</sup> (C-O stretching) while broad absorption bands were observed at 3389 cm<sup>-1</sup> (N-H stretching), 2953 cm<sup>-1</sup> (C-H stretching), 1611 cm<sup>-1</sup> (C=C stretching), 1512 cm<sup>-1</sup> (C-H bending), 1280 cm<sup>-1</sup> (C-O stretching), 1081 cm<sup>-1</sup>, 1030 cm<sup>-1</sup> (C=C stretch, primary alcohol, C-O stretch), 801 cm<sup>-1</sup> (C-O stretch, carbonate ion) corresponding to functional groups present the drug. Additional moderate to intense bands ranging between 1600-1300 cm<sup>-1</sup>, 1200-1000 cm<sup>-1</sup> and 800-600 cm<sup>-1</sup> were observed, due to the presence of hydroxy compounds that the hydrogen-bonded-OH absorption. This indicates that drug as well as neomycin sulphate loaded silver nanoparticle composite chitosan film both have similar peaks indicating that there is no interaction between drug and excipients used in formulation of film dressing.

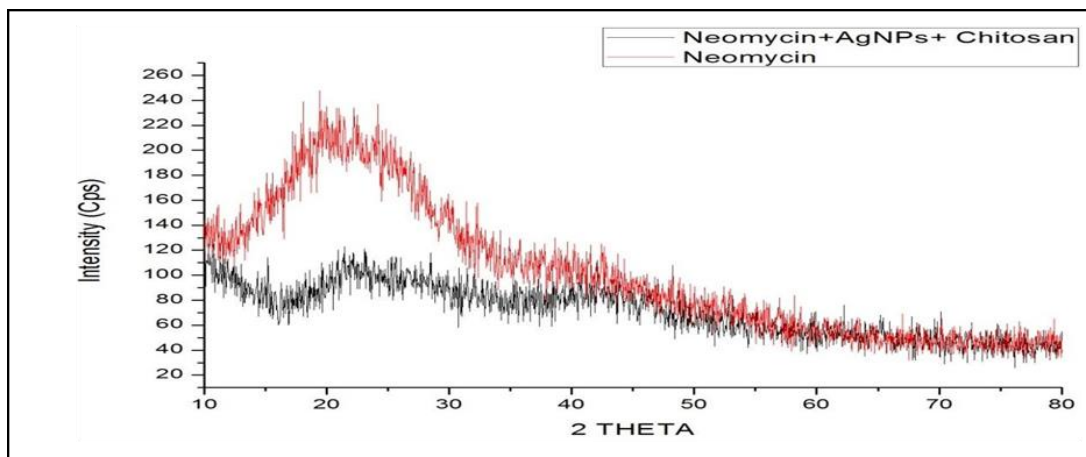


Figure 2. XRD spectra of neomycin and optimized formulation

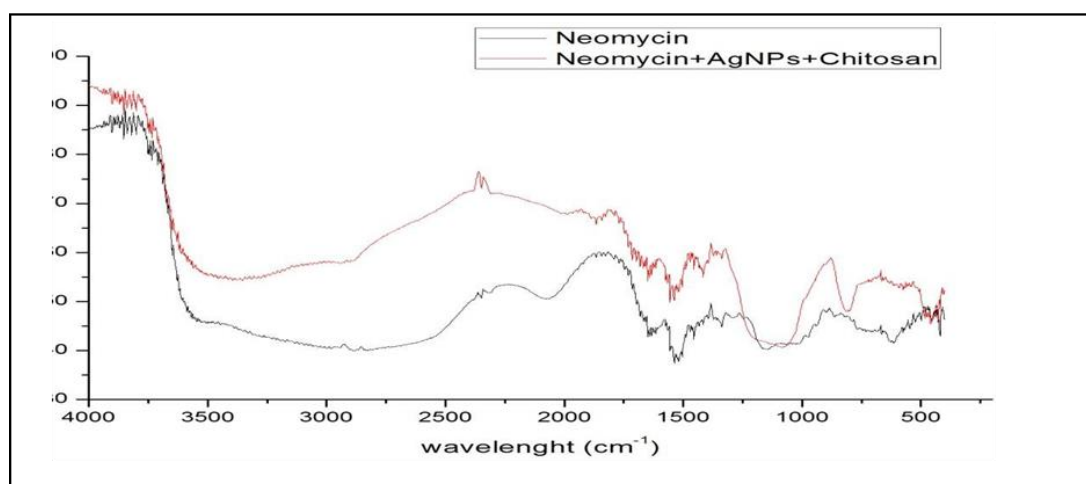


Figure 3. FT-IR spectra of neomycin and optimized formulation

### 2.9. In Vivo study

While wound contraction refers to the process of the wound's area getting smaller, wound healing activity refers to the process by which damaged tissue is returned as nearly as possible to its normal state. It primarily depends on the tissue's capacity for repair, which may be lowered as a result of burns. For comparison of the percentage of wound healing activity, pictures of various groups were taken at specific intervals (Figure 4). The wound healing efficacy of the formulation in comparison with standard and other treatment groups are depicted in Figure 4 and % wound healing is reported in Table 8. The results of statistical analysis, as depicted in table 8, indicated that, compared to control group, wound healing was remarkably improved in the groups treated with standard treatment as well as groups treated with other formulations and optimized formulation. It is also observed that wound healing was significantly improved in group treated with optimized formulation in comparison with standard group. This could be attributed to the synergistic effect of drug and AgNPs loaded in chitosan film as along with drug, both silver nanoparticles and chitosan have their own wound healing properties.

### 2.10. Histopathology

Histopathology of group treated with optimized formulation at different day indicate the internally tissue healing as well as inflammation present in skin at different time interval. The various images of histopathological study (Figure 5) indicate reduction of inflammation cell with the time. Group treated with formulation shows the remarkable improvement in wound healing. Around 20th day probably no any inflammation cell found in the animal tissue. This shows the enhanced effectiveness of the formulation.

**Table 8.** Percentage wound healing in various treatment groups

Day	Group 1 Control	Group 2 Standard	Group 3 Chitosan Film	Group 4 AgNPs + Chitosan Film	Group 5 Optimized formulation
3	02.67 ± 0.764	07.17 ± 2.255 <sup>ns</sup>	07.83 ± 1.402 <sup>**</sup>	10.67 ± 1.889 <sup>***</sup>	16.67 ± 0.983 <sup>****</sup> [#]
5	08.17 ± 1.041	16.17 ± 2.021 <sup>*</sup>	15.58 ± 1.686 <sup>***</sup>	19.67 ± 2.463 <sup>***</sup>	29.08 ± 1.429 <sup>****</sup> [##]
7	12.33 ± 1.258	26.00 ± 2.500 <sup>*</sup>	27.00 ± 1.183 <sup>***</sup>	32.17 ± 3.615 <sup>****</sup>	41.67 ± 2.714 <sup>****</sup> [##]
10	21.33 ± 2.754	36.67 ± 2.517 <sup>**</sup>	38.33 ± 2.273 <sup>**</sup>	42.50 ± 3.130 <sup>**</sup>	51.75 ± 1.605 <sup>**</sup> [#]
15	28.67 ± 3.253	52.83 ± 3.547 <sup>**</sup>	53.58 ± 2.084 <sup>**</sup>	58.00 ± 2.828 <sup>**</sup>	73.33 ± 2.639 <sup>**</sup> [#]
20	40.00 ± 2.179	64.00 ± 1.803 <sup>***</sup>	65.50 ± 1.761 <sup>***</sup>	73.25 ± 2.092 <sup>***</sup>	83.92 ± 3.338 <sup>****</sup> [###]
25	46.17 ± 2.021	75.50 ± 2.500 <sup>***</sup>	75.92 ± 2.084 <sup>***</sup>	81.92 ± 3.323 <sup>****</sup>	91.92 ± 2.691 <sup>****</sup> [##]

ns = non-significant ( $p > 0.05$ ); significant ( $*p < 0.05$ ;  $**p < 0.01$ ;  $***p < 0.001$ ;  $****p < 0.0001$ ) when compared with control; and significant [# $p < 0.05$ ; ## $p < 0.01$ ; ### $p < 0.0001$ ] when compared with standard



**Figure 4.** *In vivo* wound healing activity of various formulations.

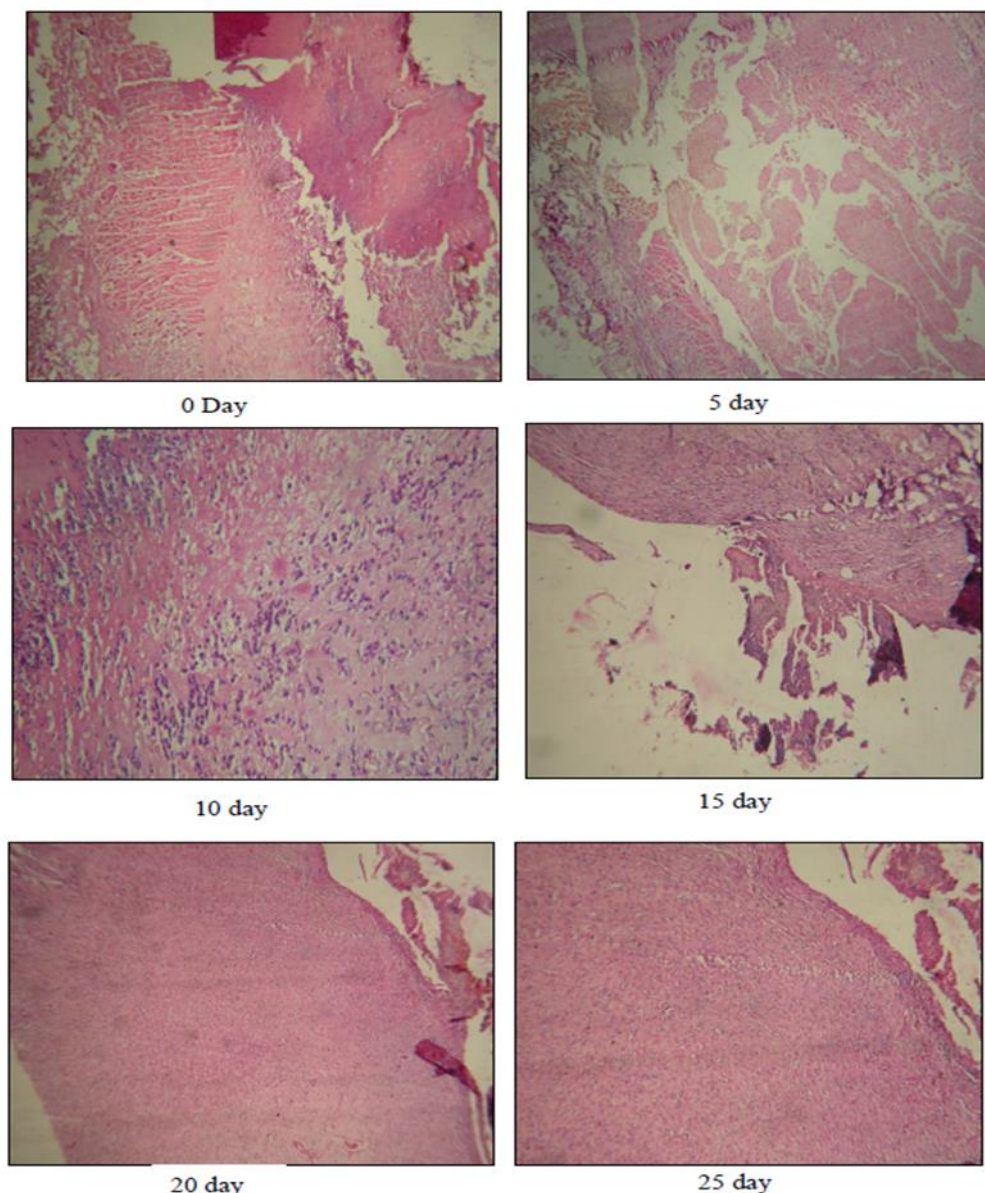


Figure 5. Histopathology of optimized formulation

### 3. CONCLUSION

This work demonstrated that silver nanoparticles prepared with SDS and polyvinyl pyrrolidone (PVP K30) are smaller and more stable and utilized in final formulation. Chitosan produced a homogenous, smooth film at a concentration of 1.4%. In comparison to neomycin sulphate and silver nanoparticle alone, neomycin sulphate drug-loaded silver nanoparticle exhibits greater antimicrobial activity. The antimicrobial activity is markedly increased by the combination of them with chitosan as later possess antimicrobial properties as well. Drug loaded silver nanoparticle-chitosan film shown a greater water absorption ability to be useful for enhancing wound healing by absorption of wound secretions. Drug containing chitosan film was more effective in wound healing in comparison with other formulation which can be attributed to its reported actions which increases the function of polymorpho nuclear cells, macrophages and fibroblastic proliferation and migration, and this was also suggested by the histopathology study. According to the *in-vivo* wound healing study, all treatment groups treated with different formulations demonstrated significantly improved wound healing compared to the control group. In addition, the optimized formulation of silver nanoparticle composite chitosan film improved wound healing significantly compared to the standard group treated with marketed formulation (cream) of silver sulfadiazine. Thus, wound healing can be improved by combining antimicrobial agents with silver nanoparticles and chitosan. So,

neomycin loaded silver nanoparticle-chitosan film can be a more effective alternative in treatment of burn wound healing.

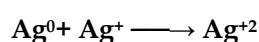
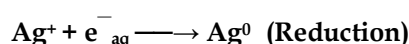
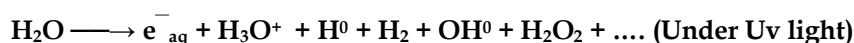
## 4. MATERIALS AND METHODS

### 4.1. Materials

Neomycin Sulphate was procured from Intas Pharmaceuticals Pvt. Ltd. Silver nitrate and chitosan were purchased from Qualigens fine chemicals, Mumbai. Sodium citrate and heavy liquid paraffin was purchased from Loba Chemie Pvt. Ltd. Sodium dodecyl sulphate, polyvinyl pyrrolidone K-30, dodecyl trimethyl ammonium bromide, cetyl trimethyl ammonium bromide,  $\beta$ -cyclodextrin, brij 35, gelatin, tween 80 and span 20 were purchased from S.D. Fine-Chemicals, Mumbai. Surgical gauze was obtained from Medicare hygiene private Ltd. Ahmedabad. Hydroxy propyl methyl cellulose K4M was procured from Colorcon, Goa. All other chemicals and reagents used in the study were of analytical grade.

### 4.2. Synthesis of Silver nanoparticle by Ultraviolet method

Several methods are available for synthesis of silver nanoparticles. Silver nanoparticles were synthesised by ultraviolet method.(32,33) Synthesis of AgNPs was by taking, 2 gm of gelatine in 190 ml of water in a flask, stir this solution till clear solution is obtained. In this gelatine solution add Aqueous  $\text{AgNO}_3$  (10 mL, 1 M) by continuous stirring to obtain  $\text{Ag}^+$ /gel-solution. Place this solution into the UV reactor for UV irradiation at different times (i.e., 1, 3, 6, 18, 24, 36, and 48 h) at room temperature. The produced solvated electrons reduce the metallic cations to the metallic atoms and finally coalesce to form agglomerates, as explained by below reactions:



### 4.3. Chemical method for Synthesis of Silver nanoparticle

Among the several chemical processes available for silver nanoparticle synthesis, chemical reduction is the most widely used due to its simplicity of application. Another important consideration is to select a suitable reducing agent, since the type of the reducing agent has a significant impact on the size, shape, and distribution of particle sizes [34]. In this study, silver nanoparticles were synthesised by chemical reduction and optimized for selection of suitable surfactant and polymer. Three round bottom flask were taken for the preparation of silver nanoparticles and were dipped into heating medium (paraffin heavy oil). The vapour generated by heating mixture was condense with the help of condenser and round bottom flask was equipped by it. In the measuring cylinder 47 ml polymer/surfactant solution was taken and 2.5 ml of 2% sodium citrate reducing agent solution was added. The prepared solution was transferred into prepared round bottom flask. Then this round bottom flask was kept in oil bath, after reaching the temperature  $90^\circ\text{C}$ , the silver nitrate solution was added drop by drop in flask while maintaining the temperature  $90^\circ\text{C}$  for one hour. After one hour the flask was removed from condenser and cooled under cold water.



For selection of appropriate surfactant, AgNPs were prepared using different surfactants including dodecyl trimethyl ammonium bromide (D-TAB), cetyl trimethyl ammonium bromide (C-TAB), sodium dodecyl sulphate (SDS), span 20, tween 80 and brij 35 at the concentration of 1%. Based on the results, SDS produced AgNPs with desired characteristics. Further, the concentration of SDS was optimized for smaller and stable nanoparticles by synthesizing AgNPs using different concentrations of SDS ranging from 5-200 mM. Synthesis of silver nanoparticles were also performed using different polymers like HPMC K4M,  $\beta$ -CD and PVP K30 for selection of suitable stabilizer.

#### 4.4. Characterization of nanoparticles

Synthesized nanoparticles were characterized for particle size determination, zeta potential measurements and UV absorbance [31, 35]. The particle size and zeta potential of silver nanoparticles were assessed by Dynamic Light Scattering (DLS) technique using a Malvern Zetasizer (Nano ZS 4800, UK). Nanoparticles dispersions were diluted sufficiently with double distilled water and analyzed at 25°C. Typically, particle sizes within the range of 10-100 nm are considered to be nanoparticles. A zeta potential of the AgNPs are indications of stability of the nanoparticles. Both sides (positive and negative) above 50 mV suggest greater nanoparticle stability. Silver nanoparticles have a yellowish-brown color in an aqueous solution due to excitation of the surface Plasmon resonance band in the UV-visible range. As a result, it exhibits a characteristic peak near 420 nm. However, because the peak changes due to preparation procedures, the solution must have a typical peak at 400-450 nm. Synthesized AgNPs were analyzed by UV-visible spectroscopy in the range of 200-800 nm using UV-visible spectrophotometer (UV-1800, Shimadzu, Japan) to observe characteristic peak of AgNPs.

#### 4.5. Preparation of Chitosan film on surgical dressing materials

Accurately weighed amount of the drug (neomycin) was taken and dissolved in the silver nanoparticles solution with continuous stirring on a magnetic stirrer. After the complete dissolution of the neomycin sulphate and fixed quantities of chitosan powder according to Table 9, glacial acetic acid was added in the final prepared solution so the final preparation contains 2% of acetic acid. The mixture was stirred continuously for 24 hours on the magnetic stirrer and then this solution was poured into the porcelain dish. The surgical dressing material was cut to a predetermined size and dipped in the porcelain dish containing above film solution. The surgical film was then removed after 5 minutes from the porcelain dish and placed on the glass plate for drying in the oven for about 3-4 hours at 60°C. Finally, drug loaded silver nanoparticles chitosan film on surgical dressing material was removed from the glass plate and subjected for evaluation of various parameters.

Table 9. Composition of chitosan films

Batch code	Chitosan Concentration
C <sub>1</sub>	1.0%
C <sub>2</sub>	1.2%
C <sub>3</sub>	1.4%
C <sub>4</sub>	1.6%
C <sub>5</sub>	1.8%
C <sub>6</sub>	2.0%

#### 4.6. Thickness of film

Uniformity in film thickness is the indication of the uniformity in content as well as drug release. The thickness of film also affect the time required to absorb the drug into the body. To determine the uniformity in thickness of film, it was measured using screw gauge at three different points of the film and the mean was reported.

#### 4.7. Content uniformity

The content uniformity of film was measured by cutting the film in size of 1 square inch at four-five different places from one film and it is placed in 25 ml of water containing beaker with continuous stirring for 24 hours. The solution is then filtered and dilution was done if required before measurement of the absorbance at 566 nm in UV spectrophotometer. Drug content in each piece of film was determined using calibration equation.

#### 4.8. Water absorption capacity

Water absorption capacity was measured which is an indication of how well drug-loaded and blank films may absorb wound exudates [36]. The pre-weighed samples of 1 sq inch were placed in 15ml of distilled water at room temperature. The weights of the expanded sections were recorded every 0.5, 1, 2, and

3 hours, and 24 hours afterwards. Percentage of the film's capacity to absorb water was assessed and calculated in triplicate using the following formula.

$$\% \text{ water absorption capacity} = \frac{(\text{Final weight} - \text{Initial weight})}{\text{Initial weight}} \times 100$$

#### 4.9. Antimicrobial assay

By using disc diffusion method, human pathogens *Escherichia coli* were used in the antibacterial assays of silver nanoparticles [37]. On Luria bertani medium plates, 100 µl of culture inoculum was disseminated using the disc diffusion method. Two conventional paper discs and a sterile paper disc containing silver nanoparticles were added to the petri plate above, where they were incubated at 37°C for 48 hours. As a control, medium devoid of silver nanoparticles was utilised. Neomycin sulphate solution, silver nanoparticle solution made from chitosan, chitosan-silver nanoparticle solution, and chitosan solution were all used in an anti-microbial assay. Gram-negative *E. coli* strain B and Gram-positive *S. aureus* bacteria were collected for the antimicrobial assay. Every sample underwent an antimicrobial assay that involved preparation and swabbing with the appropriate bacteria inoculum. Distilled water was used as a control while test samples comprised of silver nanoparticles, neomycin sulphate solution, chitosan solution, chitosan-silver nanoparticle solution, as well as silver nanoparticle-neomycin sulphate solution. Each of these plates was stored at 37°C for incubation overnight. After 24 h of incubation the zone of inhibition were measured and compared.

#### 4.10. In vitro Drug Release Study

A dissolution apparatus that is USP type-1 (basket) was used for performing in-vitro drug release study. As a dissolution medium, 900 ml of distilled water was used and the temperature was maintained at 37±0.5°C throughout the study. The films were placed in the basket of dissolution apparatus which was rotated at 100 rpm. Aliquots of 5 ml were withdrawn at predetermined time interval and the volume of the dissolution medium was kept constant by replacement with same volume of fresh media. With sufficient dilution with same media, samples were analysed by UV-Visible spectrophotometer at 566nm and the amount of the drug released at each interval was calculated using calibration equation. Percent cumulative drug release was calculated and plotted against time to get dissolution profile of the formulation.

#### 4.11. X-Ray Diffraction (XRD)

The crystalline properties of silver nanoparticles, as well as the formulation, can be determined by performing the X-Ray Diffraction of solidified formulation and silver nanoparticles. The final formulation was solidified through freeze-drying of the liquid sample followed by the addition of aerosil. The ratio of aerosil to formulation was kept 2:1. The formulation was passed through a 120# sieve after solidification to get fine solid powder of formulation. A computer-controlled Bruker AXS D8 Advance (Bruker AXS GmbH, Karlsruhe, Germany) diffractometer with an X-ray source of Ni-filtered monochromatized CuKα, Wavelength 1.5406 Å was used to perform X-Ray Diffraction. The diffraction pattern was recorded in the interval 0°<2θ<90° in a step scan mode of 0.02° per step at every 35.7 second.

#### 4.12. Fourier Transport Infrared Spectroscopy (FT-IR)

Infra-red spectra of drug in the isotropic mixtures of excipients was obtained by a FTIR-8400S spectrophotometer (Shimadzu, Japan) equipped with attenuated total reflectance (ATR) accessory. Diffuse reflectance spectroscopy (DRS)-FTIR with KBr disc was used for the analysis of pure drug neomycin sulphate and solidified formulation containing neomycin sulphate-silver nanoparticle-chitosan. Vacuum drying of all the samples is done prior to obtaining any spectra to remove the residual moisture. 32 scans were obtained at a resolution of 4 cm<sup>-1</sup> from a frequency range of 4500-400 cm<sup>-1</sup> for each spectra.

#### 4.13. In-vivo wound healing study

An *in-vivo* study was performed to check the therapeutic efficacy of the developed formulation. As the main aim of this experiment is to check the efficacy of the developed formulation on the burn wound. According to the criteria of CCSEA (Committee for Control and Supervision of Experiments on Animals) the

local Institutional Animal Ethics Committee (IAEC) of the institute has approved the protocol for the study with protocol no. 02 of 2023.

The experiment was carried out on female Wistar albino rats weighing 150-200gm and divided into 5 groups. The grouping was done according to the average weight of the rats. Numbers of animals used in each group are depicted in Table 10. One day before the development of burn injuries, the rat's backs were shaved. On the next day, rats were anaesthetized using intraperitoneal injection of Thiopental sodium (30mg/kg). Using the preheated brass rod for 60 seconds the burns were created on, opposing sides of a raised skin fold on the rat's dorsal surface. The rats were given intra-peritoneal injections of 0.5 ml sterile saline right away after the burns were made [38].

**Table 10.** Treatment protocol for *in-vivo* wound healing study

Sr. No.	Group Name	No. of Animals	Type of treatment
1.	Control Group	3	No treatment given
2.	Standard Group	3	Standard marketed formulation of silver sulfadiazine
3.	Treatment 1	6	Chitosan film treatment
4.	Treatment 2	6	Silver nanoparticle containing chitosan film treatment
5.	Treatment 3	6	Neomycin sulphate -loaded silver nanoparticles-chitosan film on surgical dressing treatment

These different treatments were given to the corresponding group's burn area after 15 minutes of cool down of the burn. The study was carried out for 25 days continuously and the dressing material was changed twice a day. Different parameters were measured for the observation of the wound healing [36]. For perceptible contrast, the photographs of wound from various groups were taken at specific intervals. The photographs of burn wound injuries were clicked at the 1<sup>st</sup>, 3<sup>rd</sup>, 5<sup>th</sup>, 7<sup>th</sup>, 10<sup>th</sup>, 15<sup>th</sup>, 20<sup>th</sup>, and 25<sup>th</sup> day of creation.

The action of repairing the injured tissue as closely as possible to its original state and wound shrinkage is called the process of wound healing. Percentage wound healing relies on the mending ability of tissue which may possibly reduce owing to burns. This parameter was measured to find the span of depletion in wound area at various timeline of treatment. The wound area was measured on 1<sup>st</sup>, 3<sup>rd</sup>, 5<sup>th</sup>, 7<sup>th</sup>, 10<sup>th</sup>, 15<sup>th</sup>, 20<sup>th</sup> and 25<sup>th</sup> day of treatment. The Extent of wound healing was calculated as % wound healing of the wound area from the original wound using a following formula:

$$\% \text{ Wound Healing} = \frac{(A_0 - A_d)}{A_0} \times 100$$

Where,  $A_0$  = Wound area on day zero and  $A_d$  = Wound area on corresponding days.

A comparison of various formulations with a control group and standard treatment groups was carried out in order to assess their effectiveness on wound healing. A two-way ANOVA with multiple comparisons was conducted on percentage wound healing data obtained for different groups in order to evaluate various formulations' effectiveness. Besides evaluating statistically significant differences between treatment groups and control group, we also investigated differences between group treated with optimized formulation and standard treatment.

Assessing the effectiveness of films in promoting wound healing requires an understanding of microscopic changes. Skin tissue samples were taken by a corneal trephiner at the first, fifth, tenth, twentieth, and twenty-fifth days following treatment in various groups to determine the level of wound healing by examining the Histopathological characteristics. 10% buffered formalin was used to preserve biopsy specimens. They underwent standard paraffin embedding procedure, which involved cutting slices that were 5 to 6 microns thick and staining them with hematoxylin and eosin. The quantity of wound healing and inflammation in rats' wound skin are shown by histopathology. Under the direction of Dr. Tarkesh Mehta, tissue histology was carried out and pictures were taken at the Blue Cross Laboratory in Nadiad. The each measurement were taken in triplicate and mean and standard deviation were calculated.

**Acknowledgements:** Authors are thankful to Dr. Shilpaben Jani, J & J Science College, Nadiad for her guidance and supervision in antimicrobial assay. Authors are also thankful to Dr. Tarkesh Mehta and Blue Cross Laboratory, Nadiad for assistance in tissue histology study.

**Author contributions:** Concept – K.S., T.S.; Design – K.S., T.S., M.P.; Supervision – T.S., M.P.; Resources – K.S., T.S., M.P.; Data Collection and/or Processing – M.B., V.P., G.U., K.P.; Analysis and/or Interpretation – K.P., K.S., T.S.; Literature Search – M.B., V.P., G.U., K.P.; Writing – M.B., V.P., G.U., K.P.; Critical Reviews – K.S., T.S., M.P.

**Conflict of interest statement:** The authors declared no conflict of interest.

## REFERENCES

- [1] Xu C, Tian LH. LncRNA XIST promotes proliferation and epithelial-mesenchymal transition of retinoblastoma cells through sponge action of miR-142-5p. *Eur Rev Med Pharmacol Sci.* 2020; 24(18): 9256–9264. [https://doi.org/10.26355/eurrev\\_202009\\_23007](https://doi.org/10.26355/eurrev_202009_23007)
- [2] Yüksel EB, Yıldırım AM, Bal A, Kuloglu T. The effect of different topical agents (silver sulfadiazine, povidone-iodine, and sodium chloride 0.9%) on burn injuries in rats. *Plast Surg Int.* 2014; 2014: 907082. <https://doi.org/10.1155%2F2014%2F907082>
- [3] Choi JS, Kim DW, Kim DS, Kim JO, Yong CS, Cho KH, Choi HG. Novel neomycin sulfate-loaded hydrogel dressing with enhanced physical dressing properties and wound-curing effect. *Drug Del.* 2016; 23(8): 2806–2812. <https://doi.org/10.3109/10717544.2015.1089958>
- [4] Alotaibi BS, Shoukat M, Buabeid M, Khan AK, Murtaza G. Healing potential of neomycin-loaded electrospun nanofibers against burn wounds. *J Drug Del Sci Tech.* 2022; 74: 103502. <https://doi.org/10.1016/j.jddst.2022.103502>
- [5] Rai M, Yadav A, Gade A. Silver Nanoparticles as a new generation of antimicrobials. *Biotech Adv.* 2008; 27(1): 76–83. <https://doi.org/10.1016/j.biotechadv.2008.09.002>
- [6] Chen X, Schluesener HJ. Nanosilver: A nanoparticle in medical application. *Tox Lett.* 2008; 176(1): 1–12. <https://doi.org/10.1016/j.toxlet.2007.10.004>
- [7] Yoon KY, Byeon J, Park JH, Ji JH, Bae G, Hwang J. Antimicrobial characteristics of silver aerosol nanoparticles against *Bacillus subtilis* bioaerosols. *Env Engg Sci.* 2008; 25: 289–293. <https://doi.org/10.1089/ees.2007.0003>
- [8] Morones JR, Elechiguerra JL, Camacho A, Holt K, Kouri JB, Ramírez JT, Yacaman MJ. The bactericidal effect of silver nanoparticles. *Nanotech.* 2005; 16(10): 2346–2353. <https://doi.org/10.1088/0957-4484/16/10/059>
- [9] Li Y, Leung P, Yao L, Song QW, Newton E. Antimicrobial effect of surgical masks coated with nanoparticles. *J Hosp Inf.* 2006; 62(1): 58–63. <https://doi.org/10.1016/j.jhin.2005.04.015>
- [10] Bruna T, Maldonado-Bravo F, Jara P, Caro N. Silver nanoparticles and their antibacterial applications. *Int J Mol Sci.* 2021; 22(13): 7202. <https://doi.org/10.3390%2Fijms22137202>
- [11] Panacek A, Kvítek L, Prucek R, Kolar M, Vecerova R, Pizúrova N, Sharma VK, Nevecna T, Zboril R. Silver colloid nanoparticles: synthesis, characterization, and their antibacterial activity. *J Phys Chem B.* 2006; 110(33): 16248–16253. <https://doi.org/10.1021/jp063826h>
- [12] Birla SS, Tiwari VV, Gade AK, Ingle AP, Yadav AP, Rai MK. Fabrication of silver nanoparticles by *Phoma glomerata* and its combined effect against *Escherichia coli*, *Pseudomonas aeruginosa* and *Staphylococcus aureus*. *Lett Appl Microbiol.* 2009; 48(2): 173–179. <https://doi.org/10.1111/j.1472-765x.2008.02510.x>
- [13] Inoue Y, Uota M, Torikai T, Watari T, Noda I, Hotokebuchi T, Yada M. Antibacterial properties of nanostructured silver titanate thin films formed on a titanium plate. *J Biomed Mater Res A.* 2010; 92(3): 1171–1180. <https://doi.org/10.1002/jbm.a.32456>
- [14] Singh R, Shitiz K, Singh A. Chitin and chitosan: Biopolymers for wound management. *Int Wound J.* 2017; 14(6): 1276–1289. <https://doi.org/10.1111/iwj.12797>
- [15] Ueno H, Mori T, Fujinaga T. Topical formulations and wound healing applications of chitosan. *Adv Drug Deliv Rev.* 2001; 52(2): 105–115. [https://doi.org/10.1016/s0169-409x\(01\)00189-2](https://doi.org/10.1016/s0169-409x(01)00189-2)
- [16] Rabea EI, Badawy ME, Stevens CV, Smagghe G, Steurbaut W. Chitosan as antimicrobial agent: applications and mode of action. *Biomacromolecules.* 2003; 4(6): 1457–1465. <https://doi.org/10.1021/bm034130m>
- [17] Li P, Poon YF, Li W, Zhu HY, Yeap SH, Cao Y, Qi X, Zhou C, Lamrani M, Beuerman RW, Kang ET, Mu Y, Li CM, Chang MW, Leong SS, Chan-Park MB. A polycationic antimicrobial and biocompatible hydrogel with microbe membrane suctioning ability. *Nat Mater.* 2011; 10(2): 149–156. <https://doi.org/10.1038/nmat2915>
- [18] Shi C, Zhu Y, Ran X, Wang M, Su Y, Cheng T. Therapeutic potential of chitosan and its derivatives in regenerative medicine. *J Surg Res.* 2006; 133(2): 185–192. <https://doi.org/10.1016/j.jss.2005.12.013>
- [19] Zhao D, Yu S, Sun B, Gao S, Guo S, Zhao K. Biomedical applications of chitosan and its derivative nanoparticles. *Polymers (Basel).* 2018; 10(4): 462. <https://doi.org/10.3390%2Fpolym10040462>
- [20] Loo HL, Goh BH, Lee LH, Chuah LH. Application of chitosan-based nanoparticles in skin wound healing. *Asian J Pharm Sci.* 2022; 17(3): 299–332. <https://doi.org/10.1016%2Fajps.2022.04.001>
- [21] Kim IY, Seo SJ, Moon HS, Yoo MK, Park IY, Kim BC, Cho CS. Chitosan and its derivatives for tissue engineering applications. *Biotechnol Adv.* 2008; 26(1): 1–21. <https://doi.org/10.1016/j.biotechadv.2007.07.009>

- [22] Xia Y, Wang D, Liu D, Su J, Jin Y, Wang D, Han B, Jiang Z, Liu B. Applications of chitosan and its derivatives in skin and soft tissue diseases. *Front Bioeng Biotechnol.* 2022; 10: 894667. <https://doi.org/10.3389/fbioe.2022.894667>
- [23] Senel S, McClure SJ. Potential applications of chitosan in veterinary medicine. *Adv Drug Deliv Rev.* 2004; 56(10): 1467-1480. <https://doi.org/10.1016/j.addr.2004.02.007>
- [24] Koide SS. Chitin-chitosan: Properties, benefits and risks. *Nutrition Res.* 1998; 18(6): 1091-1101. [https://doi.org/10.1016/S0271-5317\(98\)00091-8](https://doi.org/10.1016/S0271-5317(98)00091-8)
- [25] Kong M, Chen XG, Xing K, Park HJ. Antimicrobial properties of chitosan and mode of action: A state of the art review. *Int J Food Microbiol.* 2010; 144(1): 51-63. <https://doi.org/10.1016/j.ijfoodmicro.2010.09.012>
- [26] Andres Y, Giraud L, Gerente C, Le Cloirec P. Antibacterial effects of chitosan powder: Mechanisms of action. *Environ Technol.* 2007; 28(12): 1357-1363. <https://doi.org/10.1080/09593332808618893>
- [27] Raafat D, von Bargen K, Haas A, Sahl HG. Insights into the mode of action of chitosan as an antibacterial compound. *Appl Environ Microbiol.* 2008 ;74(12):3764-3773. <https://doi.org/10.1128%2FAEM.00453-08>
- [28] Rezvani Ghomi E, Khalili S, Nouri Khorasani S, Esmaeely Neisiany R, Ramakrishna S. Wound dressings: Current advances and future directions. *J Appl Polym Sci.* 2019; 136(27): 47738. <https://doi.org/10.1002/app.47738>
- [29] López-Miranda A,; López-Valdivieso A, Viramontes-Gamboa G. Silver nanoparticles synthesis in aqueous solutions using sulfite as reducing agent and sodium dodecyl sulfate as stabilizer. *J Nanoparticle Res.* 2012; 14(9): 1101. <https://doi.org/10.1007/s11051-012-1101-4>.
- [30] Shah VV, Bharatiya B, Mishra M, Ray D, Shah DO. Molecular Insights into sodium dodecyl sulphate mediated control of size for silver nanoparticles. *J Mol Liq.* 2019; 273, 222-230. <https://doi.org/10.1016/j.molliq.2018.10.042>.
- [31] Patel K, Bharatiya B, Mukherjee T, Soni T, Shukla A, Suhagia BN. Role of stabilizing agents in the formation of stable silver nanoparticles in aqueous solution: Characterization and stability study. *J Dispers Sci Technol.* 2017; 38(5): 626-631. <https://doi.org/10.1080/01932691.2016.1185374>
- [32] Radoń A, Łukowiec D. Silver nanoparticles synthesized by UV-irradiation method using chloramine T as modifier: Structure, formation mechanism and catalytic activity. *Cryst Eng Comm.* 2018; 20(44): 7130-7136. <https://doi.org/10.1039/C8CE01379A>
- [33] Rheima AM, Mohammed MA, Jaber SH, Hameed SA. Synthesis of silver nanoparticles using the UV-Irradiation technique in an antibacterial application. *J Southwest Jiaotong Uni.* 2019; 54(5): 34. <https://doi.org/10.35741/issn.0258-2724.54.5.34>
- [34] Iravani S, Korbekandi H, Mirmohammadi SV, Zolfaghari B. Synthesis of silver nanoparticles: Chemical, physical and biological methods. *Res Pharm Sci.* 2014; 9(6): 385-406.
- [35] Ijaz Hussain J, Kumar S, Adil Hashmi A, Khan Z. Silver nanoparticles: Preparation, characterization, and kinetics. *Adv Mater Lett.* 2011; 2(3): 188-194. <https://doi.org/10.5185/amlett.2011.1206>
- [36] Pansara C, Mishra R, Mehta T, Parikh A, Garg S. Formulation of chitosan stabilized silver nanoparticle-containing wound healing film: In vitro and in vivo characterization. *J Pharm Sci.* 2020; 109(7): 2196-2205. <https://doi.org/10.1016/j.xphs.2020.03.028>
- [37] Geoprincy G, Saravanan P, Gandhi NN, Renganathan S. A novel approach for studying the combined antimicrobial effects of silver nanoparticles and antibiotics through agar over layer method and disk diffusion method. *Digest J Nanomater Biostruct.* 2011; 6(4): 1557-1565.
- [38] Huang L, Dai T, Xuan Y, Tegos GP, Hamblin MR. Synergistic combination of chitosan acetate with nanoparticle silver as a topical antimicrobial: Efficacy against bacterial burn infections. *Antimicrob Agents Chemother.* 2011; 55(7): 3432-3438. <https://doi.org/10.1128%2FAAC.01803-10>